



## Global longitudinal strain assessment by computed tomography in severe aortic stenosis patients - Feasibility using feature tracking analysis



Miho Fukui<sup>a,1</sup>, Jeffrey Xu<sup>a,1</sup>, Islam Abdelkarim<sup>a</sup>, Michael S. Sharbaugh<sup>a</sup>, Floyd W. Thoma<sup>a</sup>, Andrew D. Althouse<sup>a</sup>, Gianni Pedrizzetti<sup>b</sup>, João L. Cavalcante<sup>a,\*</sup>

<sup>a</sup> University of Pittsburgh, Department of Internal Medicine, Division of Cardiology, Pittsburgh, PA, USA

<sup>b</sup> Department of Engineering and Architecture, University of Trieste, Trieste, Italy

### ARTICLE INFO

#### Keywords:

Computed tomography angiography  
Global longitudinal strain  
Left ventricular ejection fraction  
Aortic stenosis  
Transcatheter aortic valve replacement  
Transthoracic echocardiography

### ABSTRACT

**Background:** Global longitudinal strain (GLS) detects subclinical myocardial changes in patients with aortic stenosis (AS). Although GLS is typically measured by transthoracic echocardiography (TTE), assessment by multiphase gated computed tomography angiography (CTA) has become recently available. We sought to evaluate the feasibility of CTA-derived GLS assessment and compare its agreement with TTE using the same post-processing software in severe AS patients undergoing transcatheter aortic valve replacement (TAVR) evaluation. **Methods:** We evaluated patients with severe AS, sinus rhythm and adequate image quality for GLS analysis by both CTA and TTE pre-TAVR using 2D CT-Cardiac Performance Analysis prototype software (TomTec). The 18-segment model was used for GLS analysis by averaging the three long-axis views in both CTA and TTE studies. Agreement was assessed using linear regression and Bland-Altman analysis.

**Results:** A total of 123 consecutive patients were included (mean age  $84 \pm 7$  years, 45% female). The mean left ventricular ejection fraction (LVEF) by CTA and TTE were similar  $53 \pm 14\%$  for both. On average, CTA-derived GLS was greater than by TTE ( $-20 \pm 6.5\%$  vs.  $-16 \pm 4.9\%$ , respectively,  $p < 0.001$ ). There was a moderate correlation between GLS assessed by CTA vs. TTE ( $r = 0.62$ ,  $p < 0.001$ ), although variability between imaging methods existed. The correlation between GLS and LVEF was strong ( $r = -0.90$ ,  $p < 0.001$  for CTA,  $r = -0.88$ ,  $p < 0.001$  for TTE) using the same imaging modality.

**Conclusion:** CTA-derived GLS assessment is feasible in selected patients with sinus rhythm and adequate image quality. The agreement of GLS between TTE and CTA is moderate but not interchangeable suggesting a potential modality-specific GLS threshold.

### 1. Introduction

Aortic stenosis (AS) is a progressive disease associated with cardiac remodeling and several progressive myocardial changes.<sup>1</sup> Transcatheter aortic valve replacement (TAVR) has been a breakthrough therapeutic advance in the treatment of patients with symptomatic severe AS.<sup>2–4</sup> TAVR pre-procedural imaging planning requires acquisition of multiphase gated computed tomography angiography (CTA) for dynamic evaluation of the aortic annulus and identification of potential adverse anatomical features.<sup>5</sup> Given its high spatial resolution, accuracy, and measurement reproducibility, CTA has become the gold-standard anatomical imaging method for TAVR planning.<sup>6,7</sup>

Global longitudinal strain (GLS) quantifies myocardial deformation

and left ventricular function and has been shown to be a clinically relevant prognostic indicator in several entities,<sup>8,9</sup> including patients with severe AS.<sup>10,11</sup> GLS has been well described by transthoracic echocardiography (TTE) using speckle-tracking strain imaging<sup>12</sup> and by cardiac magnetic resonance imaging (CMR) using feature-tracking (FT) strain.<sup>13</sup> Quantification of cardiac function by CTA has been demonstrated with close correlation with CMR,<sup>14,15</sup> however this is not typically evaluated for TAVR patients. Furthermore, there is limited data regarding cardiac CTA for evaluation of GLS.<sup>16,17</sup>

In the present study, we aimed to assess the feasibility of novel FT CTA-derived GLS assessment and compare its agreement with TTE in patients with severe AS undergoing TAVR evaluation.

\* Corresponding author. Minneapolis Heart Institute, Abbott Northwestern Hospital, 800 East 28th Street, Suite 300, Minneapolis, MN, 55407, USA.

E-mail address: [joao.cavalcante@allina.com](mailto:joao.cavalcante@allina.com) (J.L. Cavalcante).

<sup>1</sup> Have equally contributed to this manuscript.

**Abbreviations:**

AS	Aortic Stenosis
CTA	Computed Tomography Angiography
FT	Feature Tracking
GLS	Global Longitudinal Strain
LVEF	Left Ventricular Ejection Fraction
TAVR	Transcatheter Aortic Valve Replacement
TTE	Transthoracic Echocardiography

**2. Methods**

**2.1. Study design**

We performed a retrospective analysis of consecutive patients with severe AS, who underwent TAVR at the University of Pittsburgh Medical Center, a large tertiary health care system, between January 2014 and December 2016. Patients underwent comprehensive clinical evaluation by the designated Heart Team and were deemed appropriate to undergo TAVR as evaluated by the guidelines. Clinical, demographic, and imaging data were prospectively collected. Patients were excluded if: a) TTE study was unable to adequately visualize  $\geq 2$  adjacent myocardial segments; b) CTA study had inadequate image quality for GLS analysis either due to poor LV blood pool contrast, significant image noise, or incomplete imaging of the left ventricle; c) presence of atrial fibrillation and/or frequent ventricular arrhythmia; or d) time between TTE and CTA study was more than 3 months.

The study was performed according to the principles of the Declaration of Helsinki and approved by the University of Pittsburgh Institutional Review Board Committee with a waiver of individual consent.

**2.2. Transthoracic echocardiogram**

A comprehensive TTE was performed before TAVR per societal guidelines using several systems (GE Vivid 7, E9, E95 [GE Medical Systems, Milwaukee, WI], and Philips iE33 [Philips Medical Systems, Andover, MA]).<sup>18</sup> Left ventricular ejection fraction (LVEF), LV end-diastolic, end-systolic and LV stroke volumes were assessed using the modified Simpson's biplane method averaging both the apical 4-chamber and apical 2-chamber views. Aortic valve was interrogated by spectral Doppler in multiple views, noting the mean and peak aortic gradients. Aortic valve area (AVA) was calculated using the continuity equation and then indexed to body surface area per guidelines.<sup>19</sup> Dedicated apical 4-, 3- and 2-chamber views with frame rate  $> 40$  frames/second were obtained and selected for GLS analysis.

**2.3. Computed tomography angiography**

TAVR CTA was performed using 64-slice multidetector computed tomography scanners (GE Lightspeed VCT64 or GE Discovery Lightspeed CT750HD, GE Healthcare, Waukesha, Wisconsin) with ECG synchronization and without dose modulation. Iterative reconstruction was used to reduce image noise while keeping radiation dose as low as reasonably achievable. A region of interest was placed within the ascending aorta at the level of the left main coronary and the scan automatically started 6 s after a threshold of 100 Hounsfield units was reached. Contrast injection rate varied according to patient's body mass index between 4 and 5 ml/s. Axial, sequential multiphase cardiac imaging with retrospective gating and minimal slice thickness of 0.6 mm was acquired at end-inspiration, following the intravenous administration of isoosmolar contrast agent on ranging between 60 and 80 ml/scan, according to patient's body mass index (Iodixanol, Visipaque 270, GE Healthcare, Waukesha, Wisconsin), followed by 50 ml to saline flush. Other scan parameters were: slice collimation

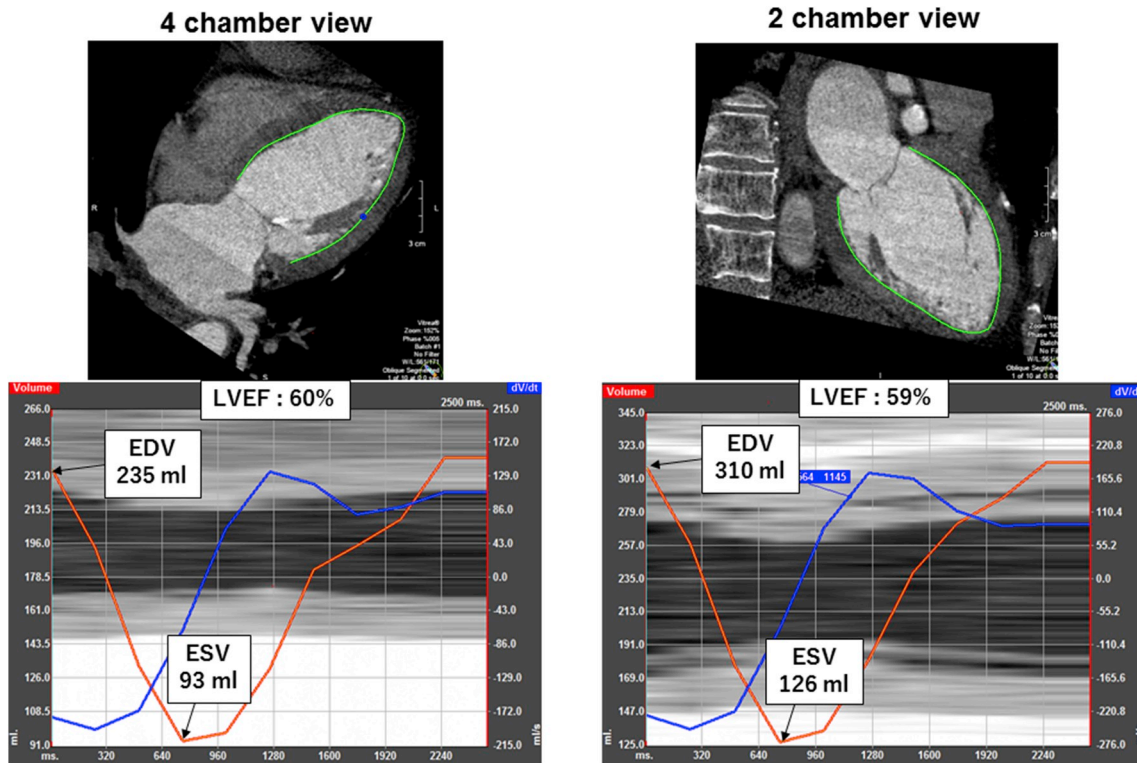


**Fig. 1.** Quantification of LV volume and LVEF using Functional CTA datasets. Similar to TTE, post-processing analysis of LVEF, LV and stroke volumes were obtained through Simpson's biplane method, using the same FT-GLS software by integrating the reconstructed 4-chamber and 2-chamber views from CTA datasets. CTA stands for computed tomography angiography; EDV, end-diastolic volume; ESV, end-systolic volume; LVEF, left ventricular ejection fraction.

width 0.625 mm, tube voltage 120 kV, peak tube current varied per patient's body mass index between 400 and 700 mAs, scan pitch varied per patient's heart rate between 0.16 and 0.24, gantry rotation time 270 msec, display field of view 180 mm and temporal resolution of 135 msec. Image series were directly reconstructed from the raw data in 10% steps throughout the entire cardiac cycle (5%–95% of the R–R interval) resulting in 10 phases per cardiac cycle with a reconstruction thickness of 0.675 mm. No routine administration of  $\beta$ -blockers and/or nitrates were used for CTA scanning purposes because of hemodynamic concerns with underlying severe AS.

Offline 3D multiplanar reconstructions were performed on a dedicated stand-alone workstation (VitreaAdvanced<sup>®</sup> 6.7.6, Vital Images, Minnetonka, Minnesota) to generate two-dimensional cine clips of 4-, 3- and 2- views, which were exported as audio video interleave (.avi) files for GLS analysis. Similar to TTE, post-processing analysis of LVEF, LV and stroke volumes were obtained through Simpson's biplane method, using the same FT-GLS software by integrating the reconstructed 4-chamber and 2-chamber views from CTA datasets (Fig. 1).

#### 2.4. Strain analysis by TTE and CTA

For GLS quantification of both TTE and CTA studies, 2D CT-Cardiac Performance Analysis (version 1.2.3.6, TomTec Imaging Systems GmbH, Unterschleissheim, Germany) prototype software analysis was used which is a vendor independent software. Manual outlining the endocardial border was performed avoiding placing points at the mitral annulus, left ventricular outflow tract areas, and papillary muscles (Fig. 2). This was followed by automated FT propagation and processing of strain analysis throughout the cardiac cycle. FT was then reviewed and, when necessary, manual adjustments of segmental contours were done to optimize tracking. The 18-segment model (6 segments per view) was used for GLS analysis by averaging the three long-axis views (2-, 3- and 4-chamber). On average, the FT-CT GLS analysis took 5–6 min per patient which was less than what it took for FT-TTE GLS analysis (8–10 min per patient). This was related to clearer endocardial border delineation on CT datasets. The longest process, however, was to load the entire multiphasic CTA dataset from PACS system into Vitrea, to evaluate the adequacy of image quality, to create and save the two-dimensional.AVI cine clips of 4-, 3- and 2- views (total process could take up to 10 min per patient).

#### 2.5. Statistical analysis

Continuous variables are summarized as mean  $\pm$  standard deviation; categorical variables are summarized as frequency and percentage. The correlation between FT-GLS derived from CTA and TTE were assessed. In addition, GLS and LVEF by both imaging modalities were also evaluated and compared using Student's paired T test. Pearson correlation coefficients were computed and agreement was assessed using linear regression and Bland-Altman analysis. A random sample of 20 patients from the study cohort was chosen to determine intraobserver and interobserver variability of CTA-derived GLS measurements using intraclass correlation coefficient (ICC). All statistical analyses were performed using SAS software version 9.4 (SAS Institute, Cary, NC).

### 3. Results

A total of 533 patients underwent TAVR at our institution during the study period, of whom 101 and 171 patients had inadequate TTE and CTA image quality respectively. Other 130 patients had significant cardiac arrhythmia at the time of CTA acquisition with degradation of imaging quality for analysis, and 8 had a time difference greater than 3 months between TTE and CTA studies. The most common reason for inadequate CTA study (22%) for GLS analysis was incomplete inclusion of the LV, since TAVR study focused in the primary evaluation of the aortic root complex. The study workflow is shown in Fig. 3.

The final study cohort included 123 patients. The mean age was  $84 \pm 7$  years, 45% female, mean Society of Thoracic Surgeons Predicted Risk of Mortality (STS-PROM) was  $7.6 \pm 4.0\%$  (Table 1). All patients had severe aortic stenosis by TTE with mean indexed aortic valve area of  $0.37 \pm 0.09 \text{ cm}^2/\text{m}^2$  and mean aortic valve mean gradient  $48 \pm 14 \text{ mmHg}$  (Table 2). The mean TTE-derived LVEF was  $54\% \pm 13\%$ .

Median time between TTE and CTA was 15 days (interquartile range: 5–27 days). Of note, there was no TAVR intervention and/or clinical event between the two imaging studies. The mean LVEF measured using Simpson's rule was similar between CTA and TTE studies. However, the LV volumes and stroke volume were significantly higher by CTA. Consequently, the mean CTA-derived GLS was greater than that by TTE (Table 3).

Inter-modality correlation of GLS measured by CTA and TTE was

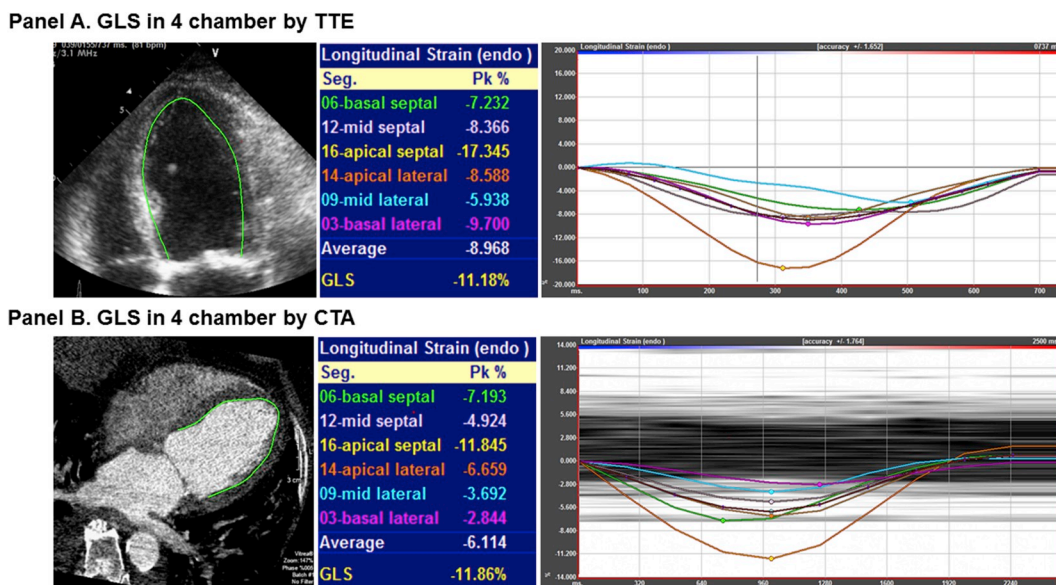
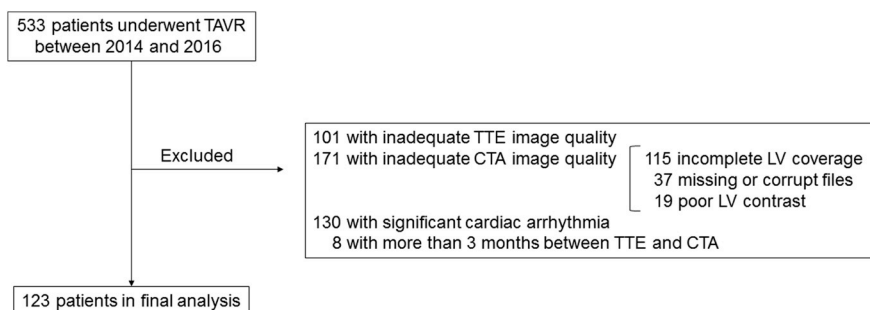


Fig. 2. Representative single view GLS analysis on same patient using 2D-CT Cardiac Performance Analysis prototype software. **Panel A** - GLS in 4 chamber by TTE. **Panel B** - GLS in 4 chamber by CTA. CTA stands for computed tomography angiography; GLS, global longitudinal strain; TTE, transthoracic echocardiography.



**Fig. 3.** Study population and workflow. A total of 533 patients underwent TAVR at our institution during the study period. A total of 410 patients were excluded for several reasons as shown, leaving 123 patients included in the final analysis. CTA stands for computed tomography angiography; TAVR, transcatheter aortic valve replacement; TTE, transthoracic echocardiography.

**Table 1**  
Baseline clinical characteristics.

Number of patients	123
Age (years)	84.2 ± 6.6
Gender	
Male	68 (55.3%)
Female	55 (44.7%)
BMI (kg/m <sup>2</sup> )	26.4 ± 5.4
Hypertension (%)	107 (87.0%)
Diabetes (%)	40 (32.5%)
Creatinine (mg/dl)	1.45 ± 1.48
NYHA class ≥ 3	102 (82.9%)
STS-PROM score (%)	7.56 ± 4.03
Prior CABG (%)	34 (27.6%)
Prior Valve Replacement (%)	6 (4.9%)

Data are expressed as mean ± standard deviation or frequency (percentage).

BMI, body mass index; CABG, coronary artery bypass graft; NYHA, New York Heart Association functional class; STS-PROM, Society of Thoracic Surgeons Predicted Risk of Mortality.

**Table 2**  
Baseline echocardiographic characteristics.

Number of patients	123
Left Ventricular Ejection Fraction (%)	54.1 ± 12.9
Interventricular Septal Thickness (mm)	13.8 ± 2.5
Left Ventricular Mass Index (g/m <sup>2</sup> )	150 ± 39
Relative Wall Thickness (%)	0.60 ± 0.17
Left Atrial Volume Index (ml/m <sup>2</sup> )	44.3 ± 13.8
Indexed Aortic Valve Area (cm <sup>2</sup> /m <sup>2</sup> )	0.37 ± 0.09
Aortic Valve Mean Gradient (mmHg)	47.8 ± 14.0
Dimensionless Index	0.20 ± 0.04
Pulmonary Artery Systolic Pressure (mmHg)	38.8 ± 14.1

Data are expressed as mean ± standard deviation.

**Table 3**  
GLS and LVEF assessment by CTA and TTE.

	CTA	TTE
GLS (%)	- 20.0 ± 6.5	- 16.0 ± 4.9*
LVEF (%)	53.1 ± 13.6	53.2 ± 13.6
LVEDV (ml)	132.6 ± 28.9	86.5 ± 32.4*
LVESV (ml)	74.7 ± 42.9	42.7 ± 24.6*
SV (ml)	84.8 ± 26.9	43.8 ± 14.2*

Data are expressed as mean ± standard deviation, \* p < 0.001 vs. CTA. CTA, computer tomography angiography; GLS, global longitudinal strain; LVEDV, left ventricular end diastolic volume; LVEF, left ventricular ejection fraction; LVESV, left ventricular end systolic volume; SV, stroke volume; TE, transthoracic echocardiography.

moderate (r = 0.62, p < 0.001) across a wide-spectrum of LVEF and shown in Fig. 4, Panel A. Bland-Altman analysis shown in Fig. 4, Panel B illustrates measurement variability, with bias of - 3.3% and 95% limits of agreement ranging between - 13.5% and 6.9%.

The relationship between GLS and LVEF measured by each modality is shown in Fig. 5. Correlation between GLS and LVEF measured by TTE was very strong (r = -0.88, p < 0.0001); the results were similar for CTA (r = - 0.90, p < 0.0001).

Intraclass correlation (ICC) for both intra-observer (ICC = 0.86) and inter-observer (ICC = 0.88) reliability for CTA-derived FT GLS measurements were excellent using the prototype software.

#### 4. Discussion

Our study has two major findings. First, feature tracking GLS analysis is feasible using retrospective gated multiphase CTA datasets in selected AS patients with adequate image quality and sinus rhythm undergoing TAVR evaluation. Second, despite a strong correlation of GLS measurements by CTA vs. TTE, variability exists between imaging methods suggesting a modality-specific GLS threshold. The additional GLS information from TAVR-CTA datasets might be prognostically helpful in AS patients with difficult TTE images and/or those with contra-indications for cardiac magnetic resonance imaging.

GLS measured by TTE has been shown to be strongly associated with outcomes in patients with aortic stenosis.<sup>20,21</sup> However, TTE-derived GLS analysis depends on proper image acquisition and adequate image quality, which can be sometimes challenging in this population.<sup>12,22</sup> GLS by CTA, on the other hand, could prove to be a useful adjunct in the evaluation of patients with poor acoustic windows by TTE and sinus rhythm. Since retrospective CTA acquisition is already routinely used for the TAVR planning, and wide-range detector scanners with full cardiac coverage continues to expand in clinical practice, there is no additional imaging acquisition required for its analysis. Nonetheless, case selection for adequate image quality and normal sinus rhythm is key for accurate post-processing GLS analysis.

The evaluation of GLS by CTA has been gaining interest but limited to small studies. Buss et al. studied 27 consecutive heart failure patients with reduced LVEF (mean LVEF: 24 ± 8%), being considered for CTA prior cardiac resynchronization therapy. The authors found a strong correlation for GLS (r = 0.84, p < 0.001) when comparing CTA vs. TTE using similar FT-GLS software, but different CT scanner technology (dual source 64-slice scanner) with improved temporal resolution. They noted that CTA's superior image quality, improved visualization and tracking of the endocardial border yielded a shorter time for GLS analysis.<sup>16</sup>

Marwan et al. recently studied 21 patients with severe aortic stenosis who had pre-post TAVR CTA imaging using 3rd generation dual-source scanner (Siemens Somatom Force, Siemens Healthineers,

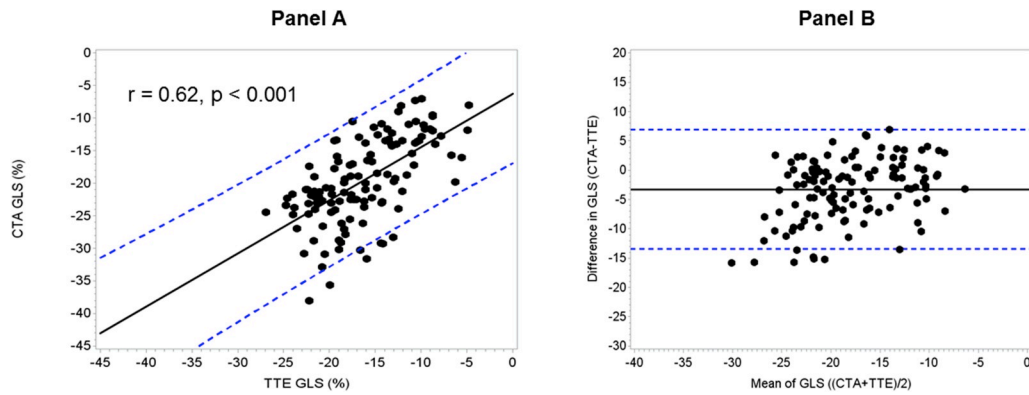


**Fig. 4.** Inter-modality correlation and agreement between CTA and TTE for GLS. Panel A - Scatterplot of CTA-derived GLS vs. TTE-derived GLS. Panel B - Bland Altman analysis for CTA-derived GLS vs. TTE-derived GLS.

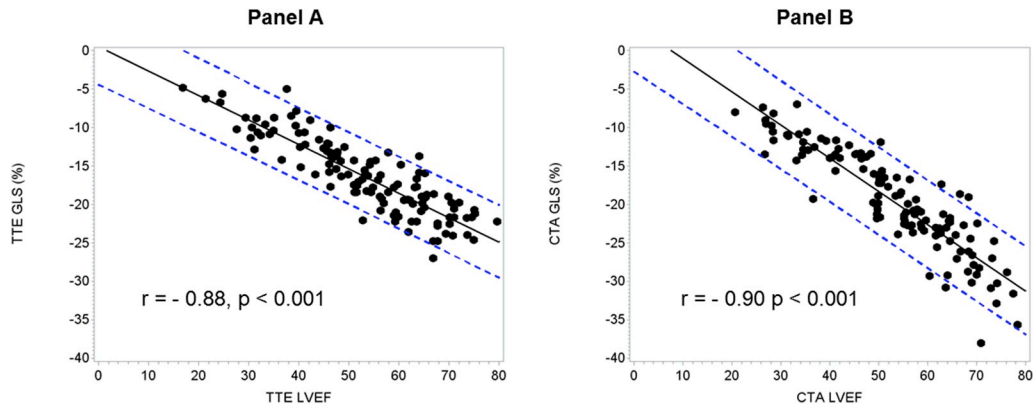


**Fig. 5.** Intra-modality correlation between GLS and LVEF Panel A - Scatterplot of TTE-derived GLS vs. TTE-derived LVEF. Panel B - Scatterplot of CTA-derived GLS vs. CTA-derived LVEF.

Forchheim, Germany; temporal resolution = 75 msec). They used a different post-processing software (Ziostation2, Ziosoft Inc, Tokyo, Japan) to obtain a maximum principal strain (3D strain), calculated using a noise-reducing motion coherence algorithm, and a perimeter derived longitudinal strain calculated by tracing the epicardial surface of the LV. A separate software was used to calculate 2D-TTE GLS (EchoPAC BT12; GE Medical Systems, Milwaukee, WI) presumably deriving peak systolic endocardial strain. Although feasibility was demonstrated, with strong correlations for both maximum principal and perimeter derived longitudinal strain when compared to TTE ( $r = -0.85$ ,  $p < 0.0001$  and  $r = 0.79$ ,  $p < 0.0001$ ), a systematic underestimation of CTA GLS was observed when compared to TTE-GLS (bias = 4.2%, 95% limits of agreement of 10.9% to -2.4%). In addition, discrete improvements in CTA-GLS were observed at post-TAVR follow-up.<sup>17</sup>

Our study builds on their data by looking at the feasibility of FT CTA-derived GLS analysis on the largest population to date with severe AS ( $n = 123$ ) evaluated by this technique and encompassing a broad range of LVEF. Importantly, we have used the same methodology and post-processing software package to measure FT GLS in both CTA and TTE datasets. Although this limited inter-vendor variability, our findings suggest that FT GLS values are modality-specific, and not interchangeable. This might be explained by the fact that FT bases the calculation of GLS from endocardial border movement and not based on the deformation of the myocardium as speckle tracking echocardiography does.<sup>23</sup> The correlation between FT-CT GLS and LVEF was very good but appears to be modest between speckle tracking echocardiography GLS and LVEF by CMR.<sup>24</sup>

A potential reason why FT-CT GLS is larger in magnitude than that measured by two-dimensional echocardiography could be related to larger left ventricular and stroke volumes measured by three-

dimensional cross-sectional modalities such as cardiac CT and MRI.<sup>25</sup> Prior intermodality comparison studies, albeit with smaller sample sizes, have reported differences between FT-GLS by CMR vs. FT-GLS by Echo.<sup>26,27</sup> Furthermore, although LVEF values were similar between the 2 modalities, GLS is load-dependent,<sup>28,29</sup> and it correlates well with LV stroke volume,<sup>30</sup> which was significantly higher by CTA vs. TTE.

Evaluation of myocardial strain by CTA continues to evolve in parallel with technological advances which have allowed single-beat full cardiac coverage and increased temporal resolution with the use of dual-source scanners.<sup>31</sup> Regional strain by tracking endocardial features from 4D cine CTA data has recently shown to be feasible, in a limited cohort of patients, across a wide spectrum of different CT scanners.<sup>32</sup>

#### 4.1. Limitations

There are limitations in this study. First, we applied a stringent inclusion and exclusion criteria which was necessary for the purposes of inter-imaging modality GLS comparison, but limits the generalizability of our findings. Notably, given the retrospective design of this study, 115/533 (22%) of patients were excluded because their reconstructed CTA images did not include the entire left ventricle, making GLS analysis not feasible. As mentioned before, wider volumetric coverage (ie:  $\geq 256$ -slice scanners) with single-beat acquisition is already being used in many TAVR centers, but not available at the time of this study inception. Second, the temporal resolution provided by the single-source 64-slice CT scanner used in this study is low (135 msec) and suboptimal for the evaluation of other deformation parameters such as strain rate and/or dyssynchrony. Although multisegment reconstruction could have been used to improve temporal resolution, it was not employed during the scan acquisition given specific requirements such as longer

breath-hold, slow and regular heart rate which are not easily achievable in this symptomatic elderly population with severe aortic stenosis. Dual-source CT scanners are increasingly being used for these patients, providing not only better image quality with less artifacts, less use of contrast, lower radiation dose and better temporal resolution.<sup>31</sup>

Therefore, it is possible that newer CT scanners can overcome most of the current limitations and potentially expand the feasibility of CTA-based analysis of myocardial strain and dyssynchrony on a more routine basis.<sup>33</sup> Unfortunately, post-TAVR CT study was not routinely done in these patients and therefore this data is not available. Third, further analysis of the prognostic utility of GLS, as well as global circumferential and radial strain is currently being investigated by our group. It is possible that baseline CT derived strain could predict improvement of LVEF and clinical outcomes post-TAVR, similar to Echo-derived GLS. However, at this point we do not have the totality of data available for inclusion in this current validation manuscript. Finally, the described novel technology forces a simplification of a 3D dataset into a 2D projection. Although this was important to assess the feasibility and validity of the method against standard 2D TTE, future technological developments, similar to what is currently available for 3D echocardiography, will be necessary to evaluate 3D strain analysis using functional CTA datasets.

## 5. Conclusions

Feature-tracking GLS analysis by multiphase CTA datasets is feasible in selected patients with severe AS, adequate image quality and sinus rhythm. The agreement of FT GLS by CTA vs TTE is moderate using single-source 64-slice CT scanner and variability exists between imaging modalities suggesting a modality-specific GLS threshold. GLS information from CTA might be helpful in patients with sinus rhythm and difficult TTE images undergoing TAVR evaluation. The prognostic value of CTA-derived GLS remains unknown and should be addressed in future studies.

## Funding sources

This research did not receive any specific grant from funding agencies in the public, commercial, or not-for-profit sectors.

## Appendix A. Supplementary data

Supplementary data to this article can be found online at <https://doi.org/10.1016/j.jcct.2018.10.020>.

## References

- Cavalcante JL. Watchful waiting in aortic stenosis: are we ready for individualizing the risk assessment? *Eur Heart J*. 2016;37:724–726.
- Reardon MJ, Van Mieghem NM, Popma JJ, et al. Surgical or transcatheter aortic valve replacement in intermediate-risk patients. *N Engl J Med*. 2017;376:1321–1331.
- Deeb GM, Reardon MJ, Chetcuti S, et al. 3-Year outcomes in high-risk patients who underwent surgical or transcatheter aortic valve replacement. *J Am Coll Cardiol*. 2016;67:2565–2574.
- Grover FL, Vemulapalli S, Carroll JD, et al. 2016 Annual report of the society of thoracic surgeons/American college of cardiology transcatheter valve therapy registry. *J Am Coll Cardiol*. 2017;69:1215–1230.
- Cavalcante JL, Schoenhagen P. Role of cross-sectional imaging for structural heart disease interventions. *Cardiol Clin*. 2013;31:467–478.
- Achenbach S, Delgado V, Hausleiter J, Schoenhagen P, Min JK, Leipsic JA. SCCT expert consensus document on computed tomography imaging before transcatheter aortic valve implantation (TAVI)/transcatheter aortic valve replacement (TAVR). *J Cardiovasc Comput Tomogr*. 2012;6:366–380.
- Otto CM, Kumbhani DJ, Alexander KP, et al. 2017 ACC expert consensus decision pathway for transcatheter aortic valve replacement in the management of adults with aortic stenosis: a report of the American college of cardiology task force on clinical expert consensus documents. *J Am Coll Cardiol*. 2017;69:1313–1346.
- Potter E, Marwick TH. Assessment of left ventricular function by echocardiography: the case for routinely adding global longitudinal strain to ejection fraction. *JACC Cardiovasc Imaging*. 2018;11:260–274.
- Park JJ, Park JB, Park JH, Cho GY. Global longitudinal strain to predict mortality in patients with acute heart failure. *J Am Coll Cardiol*. 2018;71:1947–1957.
- Kusunose K, Goodman A, Parikh R, et al. Incremental prognostic value of left ventricular global longitudinal strain in patients with aortic stenosis and preserved ejection fraction. *Circ Cardiovasc Imaging*. 2014;7:938–945.
- Kearney LG, Lu K, Ord M, et al. Global longitudinal strain is a strong independent predictor of all-cause mortality in patients with aortic stenosis. *Eur Heart J Cardiovasc Imag*. 2012;13:827–833.
- Collier P, Phelan D, Klein A. A test in context: myocardial strain measured by speckle-tracking echocardiography. *J Am Coll Cardiol*. 2017;69:1043–1056.
- Almutairi HM, Boubertakh R, Miquel ME, Petersen SE. Myocardial deformation assessment using cardiovascular magnetic resonance-feature tracking technique. *Br J Radiol*. 2017;90:20170072.
- Greupner J, Zimmermann E, Grohmann A, et al. Head-to-head comparison of left ventricular function assessment with 64-row computed tomography, biplane left cineventriculography, and both 2- and 3-dimensional transthoracic echocardiography: comparison with magnetic resonance imaging as the reference standard. *J Am Coll Cardiol*. 2012;59:1897–1907.
- Kinno M, Nagpal P, Horgan S, Waller AH. Comparison of echocardiography, cardiac magnetic resonance, and computed tomographic imaging for the evaluation of left ventricular myocardial function: Part 1 (global assessment). *Curr Cardiol Rep*. 2017;19:9.
- Buss SJ, Schulz F, Mereles D, et al. Quantitative analysis of left ventricular strain using cardiac computed tomography. *Eur J Radiol*. 2014;83:e123–130.
- Marwan M, Ammon F, Bittner D, et al. CT-derived left ventricular global strain in aortic valve stenosis patients: a comparative analysis pre and post transcatheter aortic valve implantation. *J Cardiovasc Comput Tomogr*. 2018;12:240–244.
- Lang RM, Badano LP, Mor-Avi V, et al. Recommendations for cardiac chamber quantification by echocardiography in adults: an update from the American society of echocardiography and the European association of cardiovascular imaging. *J Am Soc Echocardiogr*. 2015;28:1-39 e14.
- Baumgartner H, Hung J, Bermejo J, et al. Recommendations on the echocardiographic assessment of aortic valve stenosis: a focused update from the European association of cardiovascular imaging and the American society of echocardiography. *J Am Soc Echocardiogr*. 2017;30:372–392.
- Ng ACT, Prihadi EA, Antoni ML, et al. Left ventricular global longitudinal strain is predictive of all-cause mortality independent of aortic stenosis severity and ejection fraction. *Eur Heart J Cardiovasc Imag*. 2018;19:859–867.
- Fries B, Liu D, Gaudron P, et al. Role of global longitudinal strain in the prediction of outcome in patients with severe aortic valve stenosis. *Am J Cardiol*. 2017;120:640–647.
- Negishi K, Negishi T, Kurosawa K, et al. Practical guidance in echocardiographic assessment of global longitudinal strain. *JACC Cardiovasc Imaging*. 2015;8:489–492.
- Claus P, Omar AMS, Pedrizzetti G, Sengupta PP, Nagel E. Tissue tracking technology for assessing cardiac mechanics: principles, normal values, and clinical applications. *JACC Cardiovasc Imaging*. 2015;8:1444–1460.
- Brown J, Jenkins C, Marwick TH. Use of myocardial strain to assess global left ventricular function: a comparison with cardiac magnetic resonance and 3-dimensional echocardiography. *Am Heart J*. 2009;157:102 e101-105.
- Jenkins C, Moir S, Chan J, Rakhit D, Haluska B, Marwick TH. Left ventricular volume measurement with echocardiography: a comparison of left ventricular opacification, three-dimensional echocardiography, or both with magnetic resonance imaging. *Eur Heart J*. 2009;30:98–106.
- Aurich M, Keller M, Greiner S, et al. Left ventricular mechanics assessed by two-dimensional echocardiography and cardiac magnetic resonance imaging: comparison of high-resolution speckle tracking and feature tracking. *Eur Heart J Cardiovasc Imag*. 2016;17:1370–1378.
- Padiyath A, Gribben P, Abraham JR, et al. Echocardiography and cardiac magnetic resonance-based feature tracking in the assessment of myocardial mechanics in tetralogy of Fallot: an intermodality comparison. *Echocardiography (Mount Kisco, NY)*. 2013;30:203–210.
- Negishi K, Borowski AG, Popovic ZB, et al. Effect of gravitational gradients on cardiac filling and performance. *J Am Soc Echocardiogr*. 2017;30:1180–1188.
- Lu J, Bjorkum AA, Xu M, Gaus SE, Shiromani PJ, Saper CB. Selective activation of the extended ventrolateral preoptic nucleus during rapid eye movement sleep. *J Neurosci*. 2002;22:4568–4576.
- Cameli M, Lisi M, Mondillo S, et al. Prediction of stroke volume by global left ventricular longitudinal strain in patients undergoing assessment for cardiac transplantation. *J Crit Care*. 2011;26:433 e413-420.
- Lewis MA, Pascoal A, Keevil SF, Lewis CA. Selecting a CT scanner for cardiac imaging: the heart of the matter. *Br J Radiol*. 2016;89:20160376.
- McVeigh ER, Pourmorteza A, Guttman M, et al. Regional myocardial strain measurements from 4DCT in patients with normal LV function. *J Cardiovasc Comput Tomogr*. September–October, 2018;12(5):372–378 <http://doi.org/10.1016/j.jcct.2018.05.002>.
- Buss SJ, Schulz F, Wolf D, et al. Quantitative analysis of left ventricular dyssynchrony using cardiac computed tomography versus three-dimensional echocardiography. *Eur Radiol*. 2012;22:1303–1309.